

Frascati, November 6, 2007

Note: **L-38****OPTICAL MODEL OF THE DIPOLES FOR THE DAΦNE UPGRADE***M. Preger***1. Introduction**

Starting from fall 2007 DAΦNE will run with a modified optics aimed at increasing its luminosity by means of the “crabbed waist” concept [1], where the longitudinal size of the two beams overlap is very short due to a small horizontal size and a large crossing angle, allowing for a substantial reduction of the vertical beta function at the crossing point (IP). The potential synchrotron instabilities related to the large Piwinski angle intrinsic to this scheme are compensated by two sextupoles, one on each side of the interaction region, with the proper intensity and phase advance with respect to the IP: their effect is such that the particles of one beam cross the other one always at the minimum vertical beta, irrespective of their horizontal position.

This approach is quite different from the original project of DAΦNE, where a small Piwinski angle was obtained with a smaller crossing angle and a large horizontal beam size at the IP. The beams crossed at a total angle of  $\approx 25$  mrad and the beam separation needed to place the arcs of the two rings at a sufficient distance was yielded by four splitter magnets, one on each side of the two interaction regions. In the new scheme the crossing angle is 50 mrad and the required beam separation is reached without the splitters, thus changing the required bending angle in the last “sector like” dipoles of the arcs [2, 3, 4]: in the outer arc this bending angle is decreased by  $\approx 10\%$ , while in the inner one it is increased by about the same amount. These dipoles are therefore powered independently from the other ones (“parallel ends” connected in series as in the previous configuration) using the power supplies of the splitters.

The dipoles have been repositioned symmetrically with respect to the new bending angle, and therefore the entrance and exit angles of the beams are changed by half the difference between the original and present bending angles. In addition, as already discussed in [2, 3, 4], a slight edge focusing was also observed in the original scheme, due to the fact that the yoke of the magnet is shorter than the nominal magnet length, while the angle between the pole faces is the nominal one.

The calculations described in the following are aimed at obtaining an optical model of the dipoles which take into account these effects both for the sector and the parallel ends ones, to be used in the machine model.

**2. Description of the method**

The vertical field component on the horizontal symmetry plane of all the 16 dipoles of the collider has been measured, as extensively described in [2, 3, 4]. The maps consist of a “longitudinal scan” following the ideal trajectory of the particles in the dipole (a first straight

section, starting at a distance where the field is negligible and perpendicular to the magnet edge, a circular arc with the nominal bending radius and nominal bending angle, and a second straight section on the other side symmetric to the first one) and along several trajectories parallel to the ideal one. With this pattern of measurements one has several field values at the same longitudinal position of the particle along its reference orbit, which can be interpolated to yield the transverse field components. The scans are made in steps of 10 mm in both the longitudinal and transverse directions.

A particle with a given energy is tracked through the field map by integrating the Lorentz force and interpolating the field values nearest to each point of the calculated trajectory. The interpolation is performed by means of a second order polynomial in the transverse direction and a fourth order polynomial in the longitudinal one. Due to the symmetry of the magnet with respect to the horizontal symmetry plane, there are no horizontal and longitudinal field components in this plane and the horizontal trajectory can be calculated taking into account the vertical field component only. A particle starting at the beginning of the map with no displacement and angle with respect to the ideal trajectory ends up with no displacement and angle at the end only for one energy and only if the dipole is perfectly symmetric with respect to the radius passing through its center. Since the dipoles of DAΦNE at its startup were powered in two series (one for the electrons and one for the positrons), it was necessary that all dipoles give the nominal bending angle to the particles at the same excitation current. For this purpose all the magnets have been realized with removable end caps, which have been individually machined to yield the correct field integral. In order to find the required end cap thickness, we adopted the criterion of finding the beam energy at which the particle exits from the map with the correct bending angle, allowing for a small displacement with respect to the ideal trajectory, and requiring the energies for all the magnets to be the same. The results of this optimization are given in [3].

In order to find a machine model representing as far as possible the real field distributions, it is possible to calculate a transfer matrix (in the horizontal plane only), by tracking a first particle starting on the ideal orbit with the optimum energy, a second at a small given displacement from it, a third at a small given angle with respect to it and a fourth with a small energy deviation from the ideal one, and taking the corresponding differences between the positions and angles of the final trajectories and the first one. Calling  $\Delta x_0$  the initial displacement,  $\Delta x'_0$  the initial angle,  $\Delta p/p$  the energy deviation,  $\Delta x_f$  the final displacement and  $\Delta x'_f$  the final angle with respect to the first trajectory, the transfer matrix is:

$$M^t = \begin{vmatrix} a_{11} & a_{12} & a_{13} \\ a_{21} & a_{22} & a_{23} \end{vmatrix}$$

$$\begin{array}{lll} a_{11} = \Delta x_f / \Delta x_0 & \text{for} & \Delta x'_0 \text{ and } \Delta p/p = 0 \\ a_{12} = \Delta x_f / \Delta x'_0 & \text{for} & \Delta x_0 \text{ and } \Delta p/p = 0 \\ a_{13} = \Delta x_f / (\Delta p/p) & \text{for} & \Delta x_0 \text{ and } \Delta x'_0 = 0 \\ a_{21} = \Delta x'_f / \Delta x_0 & \text{for} & \Delta x'_0 \text{ and } \Delta p/p = 0 \\ a_{22} = \Delta x'_f / \Delta x'_0 & \text{for} & \Delta x_0 \text{ and } \Delta p/p = 0 \\ a_{23} = \Delta x'_f / (\Delta p/p) & \text{for} & \Delta x_0 \text{ and } \Delta x'_0 = 0 \end{array}$$

The “tracked” matrix  $M^t$  is then fitted with an “optical” matrix  $M^o$  consisting of two straight sections of the same length as that used in the measurements with a sector dipole in between: the dipole has the nominal bending radius and nominal bending angle, while its entrance and exit angles are left as free parameters to minimize the quantity

$$\langle \delta \rangle = \sqrt{\frac{\sum_{ij} (a_{ij}^t - a_{ij}^o)^2}{6}}$$

The magnet parameters used to fit the different kinds of dipoles are presented in Table 1.

Table 1 – Parameters of the dipoles.

	<b>Bending radius (m)</b>	<b>Length (m)</b>	<b>Bending angle (deg)</b>	<b>Straight section length (m)</b>	<b>Nominal pole face angle (deg)</b>	<b>Displacement (mm) (see Sec.5)</b>
<b>Sector long (old configuration)</b>	1.40056	1.21000	49.50000	0.69000	0	0
<b>Sector short (old configuration)</b>	1.40056	0.99000	40.50000	0.68000	0	0
<b>Parallel long</b>	1.40056	1.21000	49.50000	0.69000	24.75	0
<b>Parallel short</b>	1.40056	0.99000	40.50000	0.68000	20.25	0
<b>Sector long (new configuration)</b>	1.52861	1.20357	45.11233	0.69000	-2.19383	+2.0
<b>Sector short (new configuration)</b>	1.26974	0.99476	44.88768	068000	2.19383	+3.6

### 3. Results for the dipoles in the old configuration

Table 2 and 3 indicate the results obtained for the long sector dipoles of the outer arcs adjacent to the interaction regions and the short ones at the same position in the inner arcs. The first column indicates the serial number of the dipole, the second is the beam energy at which the beam exits the magnets with the nominal bending angle; the third column gives the difference between the diagonal elements of the tracked matrix  $a_{11}$  and  $a_{22}$ ; this difference should vanish in the case of an ideal dipole, consisting of two symmetric halves; the fourth column is the determinant of the betatron part of the tracked matrix, which should be 1 for the ideal dipole. The fifth column gives the difference between the pole face angle yielding the minimum average difference between the elements of the tracked and the optical matrix and the nominal one (see Table 1): this average difference is indicated in the sixth column.

Table 2 – Results for the sector long dipoles in the old configuration.

Serial number	Energy (MeV)	$a_{11}-a_{22}$	Det	$\beta$ (rad)	$\langle\delta\rangle$
<b>1</b>	511.62	0.00182	0.99998	0.018	0.0030
<b>2</b>	511.65	-0.00003	0.99998	0.017	0.0026
<b>3</b>	511.86	-0.00007	0.99998	0.018	0.0027
<b>4 (prot)</b>	511.70	-0.00043	1.00000	0.017	0.0024

Table 3 – Results for the sector short dipoles in the old configuration.

Serial number	Energy (MeV)	$a_{11}-a_{22}$	Det	$\beta$ (rad)	$\langle\delta\rangle$
<b>1 (prot)</b>	511.86	0.00111	0.99986	0.011	0.0020
<b>2</b>	511.69	0.00050	0.99988	0.015	0.0020
<b>3</b>	511.81	0.00036	0.99989	0.015	0.0021
<b>4</b>	511.84	0.00079	0.99984	0.014	0.0020

From Tables 2 and 3 one can verify that the beam energy at which the nominal bending is obtained is the same for the 8 magnets within  $5 \times 10^{-4}$ ; the difference between the two diagonal matrix elements is below  $1.8 \times 10^{-3}$  and the determinant equals unity to better than  $1.6 \times 10^{-4}$ . The entrance and exit pole face angles which minimize the difference between the tracked and optical matrix are within 1 mrad for the long dipoles: in the case of the short ones, three dipoles have the same pole face angle with the same spread as the long ones, while the prototype is slightly different (by less than 4 mrad). The average difference between the elements of the tracked and optical matrix is less than  $3 \times 10^{-3}$ .

Similar results have been achieved in the case of the parallel ends dipoles, as shown in Tables 4 and 5. For these 8 dipoles the spread in beam energy for nominal bending is less than  $3 \times 10^{-4}$ , with the exceptions of the long dipole n. 3 and of the short one n. 2, which have been measured before performing the last machining on the end caps and not remeasured after. Based on the experience on the other magnets, it is reasonable to believe that after the last machining their field integral is the same as the other ones [4]. The difference between the diagonal matrix elements is less than  $2.5 \times 10^{-3}$  for the long dipoles and  $1.2 \times 10^{-3}$  for the short ones. The determinant is unity to better than  $2.2 \times 10^{-4}$  and the spread of the optimum pole face angles is within 1 mrad in the case of the long dipoles, 3 mrad for the short ones. The average difference between the tracked matrix elements and the optical matrix ones is below  $4 \times 10^{-3}$  for the long dipoles, below  $2 \times 10^{-3}$  for the short ones.

Table 4 – Results for the parallel ends long dipoles.

Serial number	Energy (MeV)	$a_{11}-a_{22}$	Det	$\beta$ (rad)	$\langle\delta\rangle$
1	511.78	0.00204	0.99982	-0.017	0.0037
2	511.83	0.00108	1.00050	-0.017	0.0037
3 (not remeasured)	512.26	0.00242	0.99979	-0.017	0.0036
4 (prot)	511.92	0.00113	0.99979	-0.016	0.0034

Table 5 – Results for the parallel ends short dipoles.

Serial number	Energy (MeV)	$a_{11}-a_{22}$	Det	$\beta$ (rad)	$\langle\delta\rangle$
1 (prot)	511.86	0.00027	0.99979	-0.008	0.0020
2 (not remeasured)	511.59	0.00120	0.99980	-0.011	0.0020
3	511.91	0.00100	0.99978	-0.010	0.0020
4	511.87	0.00003	0.99982	-0.010	0.0020

#### 4. Results for the dipoles in the new configuration

As described in Section 1, the sector dipoles are used in the upgraded machine with different bending radii and angles. In order to find the best optical model, the particles have been tracked in the dipoles by scaling the measured field maps by the ratio of the old nominal bending radius to the new one. This may introduce some error in the simulation because the magnet works near the limit of the linear range at the nominal beam energy of 510 MeV and field measurements at these scaled currents are available only for few dipoles (see Section 6). Tracking has been performed starting with an initial displacement and angle with respect to the original reference system of the measurement described in Section 2. The angle is half the difference between the new and the old bending angles, positive in the case of the short dipoles and negative for the long ones. The initial displacement is the straight section length given in Table 1 times the sine of this angle. Figures 1 and 2 show the displacement of the new trajectory with respect to the old one.

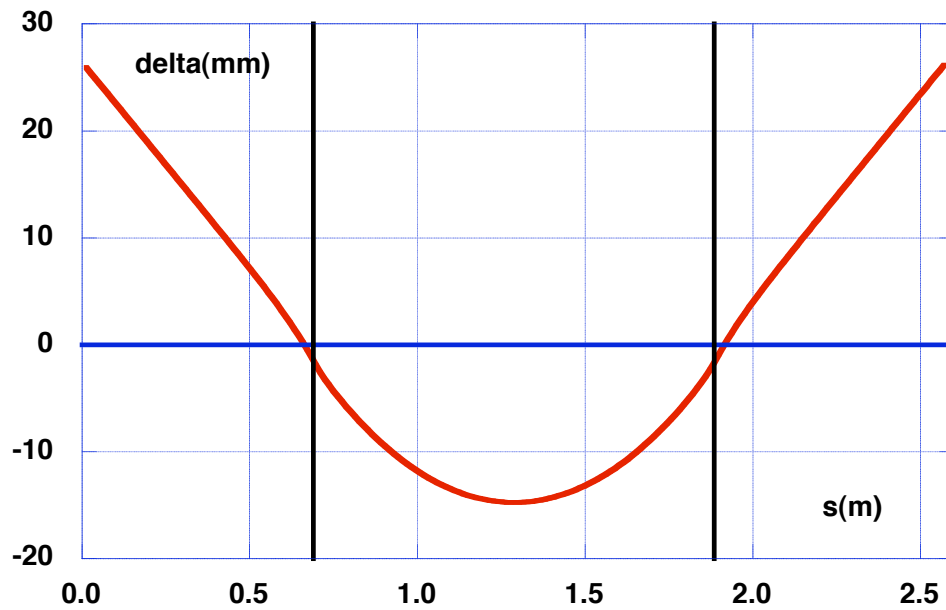


Figure 1 – Distance between beam trajectories in the new and the old configurations in the long dipoles. The black lines are at the nominal positions of the dipole pole faces.

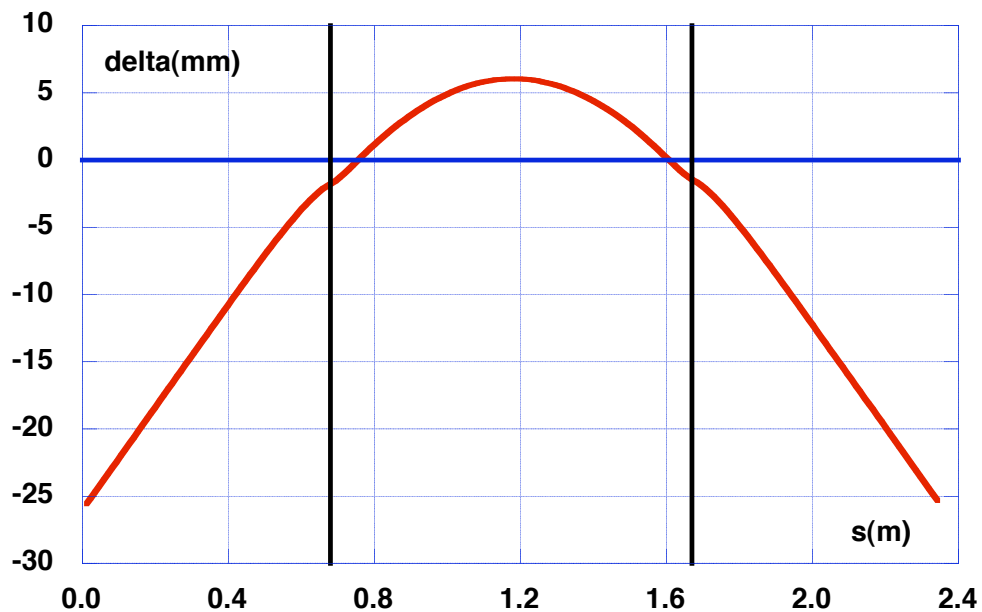


Figure 2 – Distance between beam trajectories in the new and the old configurations in the short dipoles. The black lines are at the nominal positions of the dipole pole faces.

The initial conditions have been set in such a way that a straight line with that displacement and angle crosses the nominal pole face at the center of the magnet pole. However, in the old configuration, the real trajectory of the beam is displaced towards the inside of the ring, because of the fringing field of the dipole [3]. The distance between the real and nominal trajectory (the center of the good field region) for the sector dipoles is  $\approx 3.5$  mm at the magnet center at the nominal field. In the new configuration the effect of the fringing field enhances the separation at the magnet center for the long dipoles, where the field is lower than in the old configuration, while it has the

opposite effect for the short dipoles, as shown in Figures 1 and 2. In the case of the short dipoles in the new configuration the distance between the beam trajectory and the good field region center is within  $\approx 6$  mm, with the beam on the outside of the ring. In the case of the long dipoles the beam is on the inside of the ring, the distance reaching  $\approx 12$  mm at the dipole center. To best exploit the good field region the curvature center of the short dipoles should be displaced by 3 mm towards the outside of the rings, by 6 mm towards the inside in the case of the long ones.

Table 6 – Results for the sector long dipoles in the new configuration.

Serial number	Energy (MeV)	$a_{11}-a_{22}$	Det	$\beta$ (rad)	$\langle\delta\rangle$
1	511.81	0.00133	1.00071	0.019	0.0022
2	511.82	0.00037	1.00063	0.016	0.0018
3	512.04	-0.00021	1.00071	0.018	0.0019
4 (prot)	511.86	-0.00081	1.00067	0.017	0.0018

Table 7 – Results for the sector short dipoles in the new configuration.

Serial number	Energy (MeV)	$a_{11}-a_{22}$	Det	$\beta$ (rad)	$\langle\delta\rangle$
1 (prot)	511.66	0.00097	1.00067	0.010	0.0027
2	511.48	-0.00003	1.00061	0.014	0.0027
3	511.60	0.00010	1.00072	0.014	0.0027
4	511.64	0.00070	1.00062	0.013	0.0025

Tables 6 and 7 show the results obtained for the sector dipoles in the new configuration: The spread in beam energy for nominal bending is within  $4.5 \times 10^{-4}$  in the case of the long dipoles,  $3.5 \times 10^{-4}$  for the short ones. The average energies between the two kinds of magnets differ by  $5.6 \times 10^{-4}$ . Obviously these small differences can be corrected by changing the current in the power supplies accordingly. The difference between the diagonal terms of the matrix is always within  $1.4 \times 10^{-3}$  and the maximum deviation of the determinant is  $7.2 \times 10^{-4}$ . For the long dipoles the average pole face angle fitting the tracked matrix is 17.5 mrad larger than the nominal one with a spread of 3 mrad and the average deviation between the tracked and optical matrices  $\approx 0.002$ . For the short dipoles the corresponding quantities are 11.7 mrad and 4 mrad, and the average deviation of the matrix elements  $\approx 0.003$ .

## 5. Displacement of the dipoles from the nominal position

In order to better exploit the good field region, both the short and long sector dipoles have been displaced keeping the position of the bisector fixed. The short dipoles have been moved by 3.6 mm towards the outside of the ring (see Fig. 2), the long ones by 2.0 mm in the same direction, although Fig. 1 shows that it would have been better to displace them towards the inside of the ring.

Tracking has been repeated in this new position of the magnets by performing a simple translation of the reference coordinate system. Tables 8 and 9 summarize the results in this configuration.

Table 8 – Results for the sector long dipoles in the new configuration and + 2.0 mm displacement.

Serial number	Energy (MeV)	$a_{11}-a_{22}$	Det	$\beta$ (rad)	$\langle\delta\rangle$
<b>1</b>	511.16	0.00138	1.00071	0.018	0.0022
<b>2</b>	511.17	0.00040	1.00068	0.015	0.0017
<b>3</b>	511.39	-0.00011	1.00067	0.017	0.0018
<b>4 (prot)</b>	511.21	-0.00071	1.00064	0.016	0.0016

Table 9 – Results for the sector short dipoles in the new configuration and +3.6 mm displacement.

Serial number	Energy (MeV)	$a_{11}-a_{22}$	Det	$\beta$ (rad)	$\langle\delta\rangle$
<b>1 (prot)</b>	510.47	0.00105	1.00066	0.010	0.0026
<b>2</b>	510.30	0.00000	1.00063	0.013	0.0026
<b>3</b>	510.42	0.00014	1.00062	0.013	0.0025
<b>4</b>	510.47	0.00105	1.00067	0.012	0.0025

The average energy for nominal bending decreases by 0.65 MeV in the case of the long dipoles with respect to the results obtained without the displacement, by 1.18 MeV for the short ones. The differences in the other parameters are negligible.



## 6. Excitation currents

As already mentioned in Section 4, all magnets have been measured at the nominal operation current of 266.2 A. Only three prototypes, the parallel ends short (PES), the sector like long (SLL) and the sector like short (SLS), have been measured at different currents, as shown in Table 10. The field integral has been calculated along the beam trajectory with the geometric constraints of the present configuration.

Table 10 – Field integral along the beam trajectory versus excitation current.

<b>Excitation current (A)</b>	<b>PES#1 (Tm)</b>	<b>SLL#4 (Tm)</b>	<b>SLS#1(Tm)</b>
<b>225.4</b>	1.06085	1.29189	1.06872
<b>266.2</b>	1.20688	1.46535	1.20941
<b>301.0</b>	1.29935	1.58349	1.30556
<b>354.7</b>	1.41794	-	1.42742
<b>502.9</b>	1.63825	1.99916	1.63996
<b>621.9</b>	1.74250	-	1.74197

The single beam energy at the top of the  $\Phi$  resonance, as measured by the KLOE experiment, is 509.91 MeV. This sets the required field integral for each kind of dipole, which is obtained by interpolating the values given in Table 10. The following Table 11 gives the interpolated currents for each class of dipoles: the ratio R, indicated in the third column of the Table, takes into account the difference in energy for nominal bending between the dipole measured at different currents and the average of the dipoles in the same class, as given in the Tables of the preceding Sections. The parallel ends long (PEL) dipoles are still powered in series with the short ones, and therefore their excitation current is assumed to be the same.

The required currents in the sector dipoles are quite near those of two measured field maps: for the long dipoles a map at 225.4 A is available (instead of 235.7A), for the short one we have a map taken at 301.0 A (instead of 311.7). The fitting procedure described in Section 5 has been therefore repeated on these field maps. The results are shown in Table 12, with negligible changes in the optical parameters with respect to those taken at the old nominal current.

Table 11 – Excitation currents at 509.91 MeV.

Dipole type	Required field integral (Tm)	Interpolated current (A)	R	Corrected current (A)
PES	1.20229	264.63	0.99996	264.62
SLL	1.33921	235.69	0.99996	235.68
SLS	1.33254	311.69	1.00011	311.73

Table 12 – Matrix parameters near the new operating currents.

Dipole	Excitation current (A)	Energy (MeV)	$a_{11}-a_{22}$	Det	$\beta$ (rad)	$\langle\delta\rangle$
SLL#4	225.40	491.90	-0.00103	1.00060	0.014	0.0019
SLS#1	300.95	499.58	0.00013	1.00060	0.009	0.0023

## References

- [1] P. Raimondi, D. N. Shatilov, M. Zobov: "Beam-Beam Issues for Colliding Schemes with Large Piwinski Angle and Crabbed Waist" [it.arxiv.org/abs/physics/0702033](https://arxiv.org/abs/physics/0702033).
- [2] B. Bolli, N. Ganlin, F. Iungo, F. Losciale, M. Modena, M. Paris, M. Preger, C. Sanelli, F. Sardone, F. Sgamma, M. Troiani: "The 'Short' Dipoles of the DAFNE Main Ring Achromats", MM-19, 2/8/1996.
- [3] B. Bolli, N. Ganlin, F. Iungo, F. Losciale, M. Paris, M. Preger, C. Sanelli, F. Sardone, F. Sgamma, M. Troiani: "The'Long' Dipoles of the DAFNE Main Rings Achromats", MM-25, 21/5/1997.
- [4] B. Bolli, N. Ganlin, F. Iungo, F. Losciale, M. Paris, M. Preger, C. Sanelli, F. Sardone, F Sgamma, M. Troiani: "The Dipoles of the DAFNE Main Rings Achromats", MM-26, 22/5/1997.